JOURNAL OF SYNCHROTRON RADIATION

ISSN 1600-5775

The stopped-drop method: a novel setup for containment-free and time-resolved measurements

Andreas Schiener,[a]* Soenke Seifert[b] and Andreas Magerl[a]

[a]Physics Department, Friedrich-Alexander University of Erlangen-Nürnberg, Staudtstraße 3, Erlangen 91058, Germany, and [b]X-ray Science Division, Argonne National Laboratory, 9700 South Cass Avenue, Lemont, IL 60439, USA. *Correspondence e-mail: andreas.schiener@fau.de

Received 7 July 2015
Accepted 10 December 2015

Edited by D. A. Reis, SLAC National Accelerator Laboratory, USA

Keywords: *in situ*; containment-free; millisecond time-resolved; sample environment; SAXS.

A novel setup for containment-free time-resolved experiments at a free-hanging drop is reported. Within a dead-time of 100 ms a drop of mixed reactant solutions is formed and the time evolution of a reaction can be followed from thereon by various techniques. As an example, a small-angle X-ray scattering study on the formation mechanism of EDTA-stabilized CdS both at a synchrotron and a laboratory X-ray source is presented here. While the evolution can be followed with one drop only at a synchrotron source, a stroboscopic mode with many drops is preferable for the laboratory source.

1. Introduction

Over the last decades the scientific and industrial interest in the controlled fabrication of nanostructures has increased tremendously due to their unique physical and chemical properties (Alivisatos, 1996). In this context, nanoparticles hold promise for a large variety of applications due to the size dependence of their properties when the particle radius is of the order of a few nanometres (Brus, 1986; Trindade *et al.*, 2001). However, to develop efficient reaction pathways for controlled particle synthesis routes, a fundamental understanding of the nucleation and growth process is mandatory (Baumgartner *et al.*, 2013). *In situ* X-ray diffraction and spectroscopic measurements are powerful tools for obtaining direct insight into the relevant process paths (Abécassis *et al.*, 2007).

The availability of highly intense synchrotron X-ray radiation sources of the third generation made *in situ* X-ray scattering experiments on the formation of nanoparticles accessible to a large community (Abécassis *et al.*, 2007; Narayanan, 2009; Marmiroli *et al.*, 2010), and small-angle X-ray scattering (SAXS) with a time resolution well below 1 s has become a common tool for obtaining access to the concentration and shape of particles in the size range from 1 nm up to 100 nm (Sivia, 2011).

Various *in situ* setups have been developed that are suitable for reactions in solid, liquid and gaseous environments (Schmelzer *et al.*, 2000; Beaucage *et al.*, 2004; Narayanan, 2009). Among them, commercially available stopped-flow cells are a frequently used tool to access chemical reactions in solution (Narayanan *et al.*, 2001). Here the reactants are brought together in a mixer and injected into a capillary where the flow is stopped. Typically, time-resolved experiments can be started after a dead-time of a few tens of milliseconds.

A serious disadvantage of stopped-flow setups is the risk of a time-dependent capillary coating, when chemical or physical

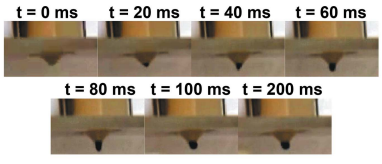

reactions take place which may influence the signal in both scattering and spectroscopic analysis techniques, particularly when the scattering is weak like it is for the case of highly diluted solutions. Possible influences are: (i) the capillary background, which has to be subtracted/corrected for, changes as a function of time which may be difficult to correct in the data reduction; (ii) owing to the coating the reactant concentrations in the solutions are changed; and (iii) the presence of the surface coating may influence the investigated reaction by, for example, initiating a needle-like growth of the reactants at a polar interface, as is known for ZnO (Wang *et al.*, 2004).

To overcome these shortcomings, free-jet setups have been developed and were used to study nucleation and growth of nanoparticles of gold (Au) (Polte *et al.*, 2010), calcium carbonate ($CaCO_3$) (Marmiroli *et al.*, 2009) and CdS (Schiener *et al.*, 2013, 2015). However, these experiments have a high reactant consumption and waste production, as the jet runs continuously. Furthermore, the upper limit of the accessible reaction time is limited to below 1 s. It is a function of the jet velocity v and the distance d between the mixing point and the observation point according to

$$t_{\rm react} = d/v. \quad (1)$$

For large d and low v the jet becomes instable due to surface waves, which results in the droplet decay of the free jet. These droplets have a significant background signal arising from surface reflections when they move through the beam. Although setups have been developed where this time window is extended using a delay tube or reservoir for the mixed chemicals before the jet creation (Polte *et al.*, 2010), it may be suspected that containers and tubes become continuously coated and the reaction conditions may still be altered.

In the following, we report on a novel method that enables time-resolved containment-free experiments at a free liquid drop starting at 100 ms after initiating the reaction for an extended time scale (up to hours).

2. Experimental

The contribution from a capillary coating in the SAXS regime in an experiment on nucleation and growth of CdS nanoparticles in a stopped-flow setup (BioLogic SF 400) is demonstrated in Fig. 1. The red circles show the background signal of a clean borosilicate capillary filled with water used as solvent for the particle reaction. The green triangles show the background of the same capillary filled again with water but after 40 stopped-flow injections of reactants of stabilized CdS. The capillary was cleaned with water after the injections. The CdS particle formation process was realised by bringing together 12.5 m*M* aqueous solutions of sodium sulfide (Na_2S) with a stoichiometric 12.5 m*M* mixture of cadmium chloride ($CdCl_2$) and EDTA (ethylenediaminetetraacetic acid disodium salt dihydrate) (Kozhevnikova *et al.*, 2010) yielding a 6.25 m*M* CdS solution. The exposure times for both data sets were 10 s at the Austrian SAXS beamline at the ELETTRA synchrotron near Trieste in Italy. The time between two

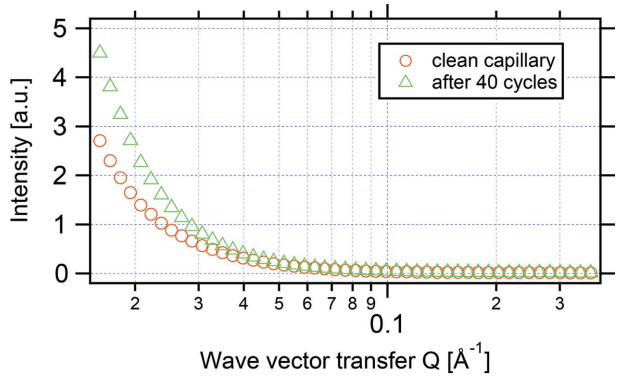

Figure 1
SAXS intensity of a water-filled borosilicate capillary of a stopped-flow device as a function of the wavevector transfer Q measured at the Austrian SAXS beamline at ELETTRA. The red circles show the measured background intensity of a clean capillary (after rinsing with a diluted HCl solution and water), while the green triangles show data after 40 injection cycles [c(CdS) = 6.25 mM = c(EDTA)] and cleaning with water after the last cycle. The difference between the two data sets originates from CdS coating of the capillary. Note that there is also a faint yellow colouration visible on the capillary. The time between each injection was 140 s; the exposure times of both SAXS data sets were 10 s.

injections was set to 140 s. The data show a significant background signal, in particular in the low Q-range. Simultaneously the capillary coating became visible as yellow film on the capillary wall. Although it is possible to acquire a water background between each injection cycle, the time-dependent coating during each cycle changes the SAXS background, and cannot be properly subtracted, as long as its kinetics are unknown. Thus, it is difficult to follow the formation process of EDTA-stabilized CdS nanoparticles *in situ* without the influence of the containment coating as systematic error.

In the following we describe a novel setup without any containment in the pathway of the incident and the scattered X-ray beam (for SAXS).

Fig. 2(*a*) shows the schematics of the stopped-drop setup, suitable for time-resolved SAXS experiments at a free liquid drop. The reactants are brought together in a Y-shaped micro mixer (custom-made out of one piece of polyether ether ketone) driven by syringe pumps (ChemYX Nexus 6000). The feeding channels (typical diameter of 100 µm) meet at an angle of 45° at the top of the mixing nozzle, where the injected solutions are mixed during infusion. At the start, the channels of the mixer are filled with the reactant solutions, while the nozzle is empty. The infusion is started *via* the remote-controlled syringe pumps. Once the reactant volume of one drop is mixed (typical volumes of a few tens of µl), the infusion is stopped and the drop remains attached *via* adhesion forces to the special shaped mixing nozzle (the size of the drop can be altered by using various nozzle shapes; for the experiments presented it was adapted to make a drop with a diameter of 3 mm). The drop formation is achieved after a dead-time of about 100 ms (which equals the mixing time of the drop) and the drop is available for SAXS experiments. With typical infusion rates of the syringe pumps of 4 ml min^{-1} a mean fluid velocity of the reactants of about 8 m s^{-1} is calculated using the diameter of 100 µm of the feeding channels. A high-speed

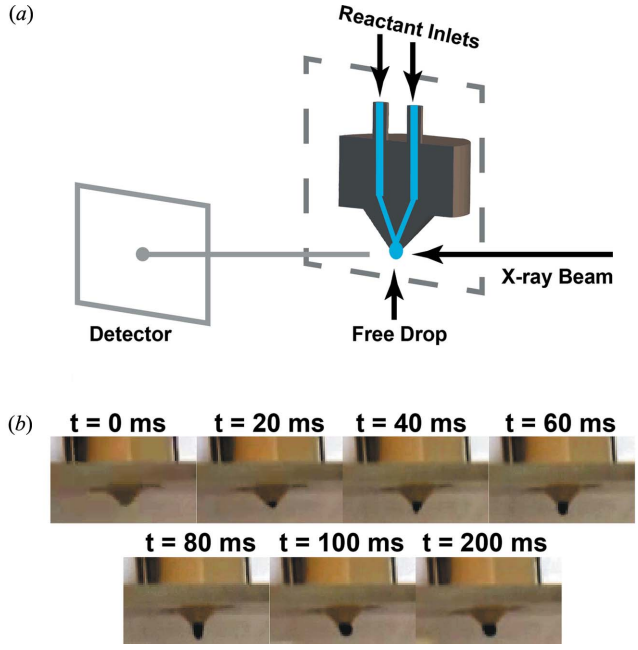

Figure 2
(*a*) Schematic of the stopped-drop SAXS experiment. The reactants are brought together in a micro mixer (see cross section of the mixer), driven by syringe pumps. Once the volume of one drop is infused, the pumps are stopped and the drop remains attached to the mixing nozzle due to adhesion forces. Time-resolved data can be acquired as soon as a stable drop is formed after 100 ms. (*b*) Series of frames acquired with a high-speed camera, showing the drop formation. The water used for this visualization is coloured with ink.

camera movie of the mixing process of water and water marked with ink shows no inhomogeneity of the drop colour during its formation. Thus, the mixing is considered as homogeneous on a sub-millimetre length scale. Fig. 2(*b*) shows a series of frames during a water drop creation (marked with ink for a better contrast of the drop), which approves the formation of the drop within 100 ms. Neither the start nor the stop processes of the syringe pumps or any spreading of the feeding channels from the syringes to the mixer have a significant influence on the formation time of the drop. After the experiment the reactant inlet channels were purged by a fast infusion of the syringe pumps and the remaining fluid in the mixing nozzle was removed instantly using a constant airflow. To prevent the environment from contamination with the used chemicals, the entire experiment takes place in a totally encapsulated chamber. Furthermore, a saturated humidity in this chamber prevents the evaporation of the drop.

The stopped-drop setup was used both in a laboratory-based SAXS setup at the physics department of the Friedrich-Alexander University in Erlangen and at two dedicated SAXS beamlines in sector 12 (12 ID-B and 12 ID-C) of the Advanced Photon Source (APS) at the Argonne National Laboratory using the same reaction settings (mixer geometry, injection velocity, reactant concentrations and injected volume). The EDTA concentrations were equal to the CdS concentrations as described above.

Two-dimensional (2D) area detectors were used for all SAXS experiments. The data reduction of the 2D images into 1D intensities as a function of the wavevector transfer Q was performed *via* the *Igor* (wavemetrics) extension *Nika* (Ilavsky, 2012) and the modelling to these SAXS intensities *via* the *Igor* (wavemetrics) extension *Irena* (Ilavsky & Jemian, 2009).

2.1. Laboratory source based stopped-drop SAXS experiments in a stroboscopic mode

The laboratory X-ray source based time-resolved stopped-drop experiments were performed at a SAXS instrument in Erlangen featuring a micro-focus Cu anode (photon energy 8 keV) and a Pilatus 300k (Dectris) 2D area detector. The CdS formation was repeated 20 times by creating 20 drops. The reaction was followed for 300 s. Individual images were accumulated for 1 s and then stored with a readout time of 10 ms. The data acquisition was started manually before the drop creation, which results in an uncertainty of the reaction time of 1 s. In this stroboscopic mode the acquired SAXS intensities were averaged for the 20 repetitions of the experiment and for 20 time frames corresponding to a time resolution of 20 s to provide a sufficient data quality for further data modelling.

2.2. Synchrotron-based stopped-drop SAXS experiments with a high time-resolution

The synchrotron-based experiments were realised at the APS 12 ID-B station (photon energy E = 14 keV). A pilatus 2M (Dectris) 2D area detector was used for data acquisition. One single drop was sufficient to acquire the total series of data points. The exposure time for each pattern was set to 100 ms. The delay times between measurements were set to 200 ms for the first 20 frames and to 500 ms, 3 s and 5 s for the following sets of 20 frames. The drop formation was again generated manually after starting the data acquisition. The drop creation is indicated by a significant decrease of the simultaneously acquired beamstop intensity between two frames, which results in an uncertainty of the reaction time of 100 ms. Although images acquired with a high-speed camera still show a slight vibration of the drop between 100 and 200 ms, the SAXS background was properly reducible for this first data point.

2.3. Synchrotron-based stopped-drop SAXS experiments for long reaction times

The synchrotron-based stopped-drop experiments on an extended time scale (several minutes) were realised at the APS 12 ID-C station (photon energy E = 12 keV) with a 2D CCD area detector. Similar to the previous section only one drop was needed to acquire the entire series of data points. The exposure time for each pattern was set to 100 ms and the time between two frames was 3 s, due to the detector specific readout time. The drop was generated manually, which results in an uncertainty of the reaction time of 1 s.

3. Results and discussion

Fig. 3 shows representative SAXS patterns (red squares) from APS 12 ID-C for the reaction times of (*a*) 1 s and (*b*) 22 s. A bimodal lognormal-distributed spherical particle model [as was already observed for CdS nanoparticles (Kozhevnikova *et al.*, 2010; Schiener *et al.*, 2015) and similar model systems like CdSe (Abécassis *et al.*, 2015)] together with a linear background (grey lines in Fig. 3) was appropriate to fit the data (black lines). The contributions of the larger population to the scattered intensities are represented by the dashed blue lines in Fig. 3, while the dashed green lines represent the scattered intensities of the smaller particles.

Fig. 4(*a*) shows the evolution of the mean radii as a function of time for the formation of EDTA-stabilized CdS nanoparticles, with a concentration of c = 6.25 mM, described by lognormal-distributed bimodal spherical particle populations. The squares and the circles correspond to the larger particle population and to the small fraction, respectively. The green data were acquired at the APS 12 ID-C station with a frame rate of 0.33 Hz in a time range from 1 s up to about 292 s; the red data acquired at the laboratory source reproduce the synchrotron data well considering their significantly larger errors. Due to the lower statistics, the size of the small population was fixed during the data modelling of the laboratory data to the mean value of the fitting results for the small particle population of the synchrotron data. Fig. 4(*b*) shows the mean radii of an experiment with half the CdS and EDTA concentration (c = 3.13 mM) acquired at APS 12 ID-B using a Pilatus area detector with a fast readout of 100 ms to achieve a time resolution of 200 ms.

The time dependence of the mean radii shows a good agreement between the laboratory-based and synchrotron-based experiments, proving the reproducibility of the reaction and the experiment. For each experimental run, the reactant solutions were prepared individually. It might be suspected that radiation damage at the synchrotron sources influences

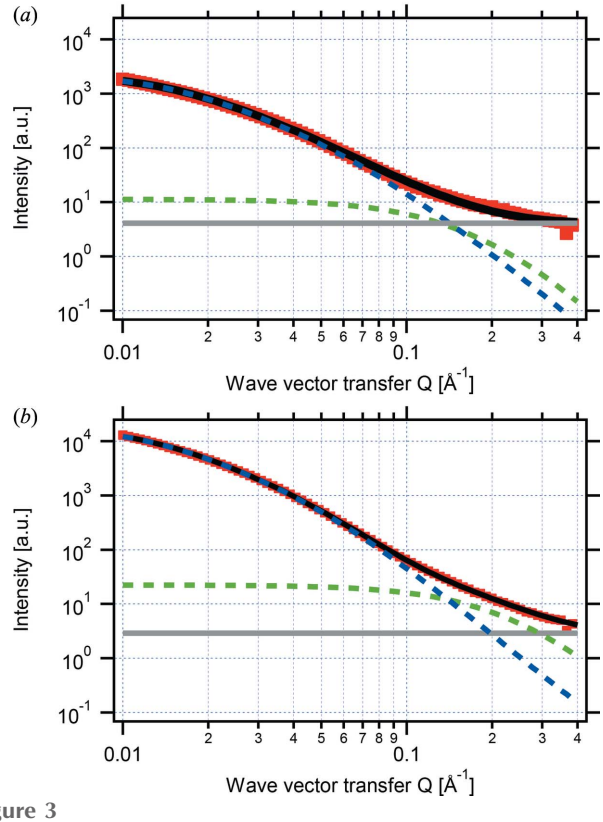

Figure 3
Reduced SAXS intensities (red squares) after 1 s (*a*) and 22 s (*b*) of EDTA-stabilized CdS formation [*c*(CdS) = 6.25 m*M*]. The patterns were acquired at the APS 12 ID-C station with an X-ray energy of 12 keV and exposure times of 100 ms. Lognormal-distributed bimodal spherical particle models together with a linear background appeared appropriate to fit the data. The dashed lines show the contributions to the scattered intensities of each population, while the black lines represent the fitting results.

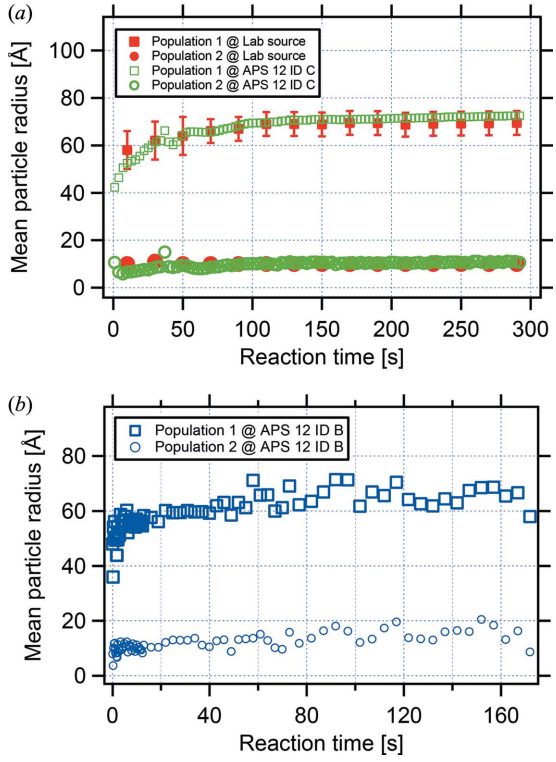

Figure 4
(*a*) Mean radii of the EDTA-stabilized CdS particles (c = 6.25 mM) as a function of reaction time. The synchrotron data (green markers) acquired at the APS 12 ID-C station show a bimodal size distribution. The small particle population has a particle radius of about 7 Å (circles) after 10 s, which is slightly increasing up to 11 Å as a function of time. In the observed time range from 1 to 292 s the larger population (squares) shows a significant increase of the mean particle radius from 40 up to 70 Å. The stroboscopic acquired laboratory data (red markers) reproduce the observed growth mechanism. To achieve this about 20 drops were measured in a stroboscopic mode and a time averaging of 20 s was necessary to achieve a proper data quality. This results in an exposure time of 400 s for each point. In order to achieve a proper data modelling, the size of the small particle population was fixed to 10 Å in radius. (*b*) Mean radii of the EDTA-stabilized CdS particles (c = 3.13 mM) as a function of reaction time. Using a Pilatus area detector featuring a fast readout (about 100 ms) at the APS 12 ID-B station, a time resolution down to 200 ms was achieved with an initial dead-time of 100 ms. The experiment reproduces the main conclusions of the experiments at the laboratory source and the APS 12 ID-C station for the half CdS concentration.

the particle formation process, because the synchrotron data shown in Fig. 4(*a*) still show a slight increase in particle size, while the laboratory data do not show a significant change in the particle size at that time scale. However, the fitting results of the synchrotron experiments would also describe the laboratory data sufficiently, because of their large experimental error bars due to lower counting statistics.

These results show that the use of the stopped-drop setup allows *in situ* experiments with significantly reduced influences of containment coatings which may be highly relevant in the case of weakly scattering samples.

(1) The background, which has to be subtracted/corrected for, has no time dependency because there is no reactant–containment interface in the beam path. This allows the acquisition of data sets with a higher data quality and reliability.

(2) The change of the initial reactant concentrations due to a containment coating is reduced because of the decrease of the ratio between the containment–reactant interface and the reaction volume A/V at the mixing nozzle in comparison with a capillary-based setup. Assuming that the drop is of spherical shape with a radius r and about one-third of its surface area is in contact with the nozzle, the ratio between the contact area A per reaction volume V is given by

$$\frac{A}{V} = \frac{4r^2\pi/3}{4r^3\pi/3} = \frac{1}{r}. \qquad (2)$$

This results, for a drop with a radius of 1.5 mm, in a ratio A/V of the stopped-drop experiment of 666 m^{-1}. Note that the drop radius is substantially influenced by the curvature of the mixing nozzle, which is an essential tool to define the drop diameter. For a capillary-based stopped-flow experiment with typical inner capillary radius r_{cap} of about 300 µm, the A/V ratio is calculated according to

$$\frac{A}{V} = \frac{2r\pi h}{r_{cap}^2\pi h} = \frac{2}{r_{cap}} \qquad (3)$$

to be 6666 m^{-1}, which is one order of magnitude larger than the value for our stopped-drop experiment.

(3) The influence on the formation mechanism based on the presence of a coated surface has two aspects. (i) The disturbed formation of particles close to a coated surface, which are linked to that surface; the influence of those will be negligible because, similar to point (1), the X-ray beam does not pass a containment–reactant interface. (ii) The particles formed under disturbing conditions, which can leave the surface into the solution. This again is a A/V-dependent effect, which is reduced by one order of magnitude for the stopped-drop experiment as compared with the stopped-flow experiment.

4. Conclusion

With the stopped-drop setup we present a novel experimental technique for containment-free time-resolved experiments as demonstrated in this article for SAXS experiments on the growth of EDTA-stabilized CdS nanoparticles. This setup is suitable both for laboratory-based stroboscopic experiments due to a high repetition rate of the drop formation of up to 5 Hz and for direct time-resolved acquisition using one single drop only at a synchrotron source. We note that each drop requires only a few µl reactant volumes, which supports experiments where the reactants are limited, expensive or where a special waste disposal procedure may be complicated to be established.

Compared with a stopped-flow device, no containment–reactant interface is in the beam path and as a consequence no background correction for a container is required. The dead-time for the formation of a stable drop is 100 ms. The drop is located in an enclosed chamber with saturated humidity which allows for long time experiments.

This method has the potential to increase significantly the data quality of *in situ* experiments for various sample systems. Beyond the application in SAXS experiments, the presented setup can be used for a broader field of experiments, *e.g.* wide-angle X-ray scattering (WAXS), total scattering (PDF) or various spectroscopic experiments.

Acknowledgements

We gratefully acknowledge funding by the German Research Foundation (DFG) through Priority Program SPP1415 and support by the Graduate School GRK 1896. Furthermore, we acknowledge Torben Schindler and Ella Schmidt for experimental support at the laboratory source in Erlangen, Heinz Amenitsch for experimental support at the Austrian SAXS beamline at ELETTRA, and the APS 12 ID beamline staff. This research used resources of the Advanced Photon Source, a US Department of Energy (DOE) Office of Science User Facility operated for the DOE Office of Science by Argonne National Laboratory under Contract No. DE-AC02-06CH11357.

References

Abécassis, B., Bouet, C., Garnero, C., Constantin, D., Lequeux, N., Ithurria, S., Dubertret, B., Pauw, B. R. & Pontoni, D. (2015). *Nano Lett.* **15**, 2620–2626.
Abécassis, B., Testard, F., Spalla, O. & Barboux, P. (2007). *Nano Lett.* **7**, 1723–1727.
Alivisatos, A. P. (1996). *Science*, **271**, 933–937.
Baumgartner, J., Dey, A., Bomans, P. H. H., Le Coadou, C., Fratzl, P., Sommerdijk, N. & Faivre, D. (2013). *Nat. Mater.* **12**, 310–314.
Beaucage, G., Kammler, H. K., Mueller, R., Strobel, R., Agashe, N., Pratsinis, S. E. & Narayanan, T. (2004). *Nat. Mater.* **3**, 370–373.
Brus, L. (1986). *J. Phys. Chem.* **90**, 2555–2560.
Ilavsky, J. (2012). *J. Appl. Cryst.* **45**, 324–328.
Ilavsky, J. & Jemian, P. R. (2009). *J. Appl. Cryst.* **42**, 347–353.
Kozhevnikova, N. S., Vorokh, A. S. & Rempel', A. A. (2010). *Russ. J. Gen. Chem.* **80**, 391–394.
Marmiroli, B., Grenci, G., Cacho-Nerin, F., Sartori, B., Ferrari, E., Laggner, P., Businaro, L. & Amenitsch, H. (2009). *Lab Chip*, **9**, 2063–2069.
Marmiroli, B., Grenci, G., Cacho-Nerin, F., Sartori, B., Laggner, P., Businaro, L. & Amenitsch, H. (2010). *Nucl. Instrum. Methods Phys. Res. B*, **268**, 329–333.
Narayanan, T. (2009). *Curr. Opin. Colloid Interface Sci.* **14**, 409–415.
Narayanan, T., Diat, O. & Bösecke, P. (2001). *Nucl. Instrum. Methods Phys. Res. A*, **467–468**, 1005–1009.

Polte, J., Erler, R., Thünemann, A. F., Emmerling, F. & Kraehnert, R. (2010). *Chem. Commun.* **46**, 9209–9211.
Schiener, A., Magerl, A., Krach, A., Seifert, S., Steinrück, H.-G., Zagorac, J., Zahn, D. & Weihrich, R. (2015). *Nanoscale*, **7**, 11328–11333.
Schiener, A., Wlochowitz, T., Gerth, S., Unruh, T., Rempel, A., Amenitsch, H. & Magerl, A. (2013). *MRS Proc.* **1528**, mrsf12-1528-vv10-04.
Schmelzer, J., Lembke, U. & Kranold, R. (2000). *J. Chem. Phys.* **113**, 1268.
Sivia, D. S. (2011). *Elementary Scattering Theory*. Oxford University Press.
Trindade, T., O'Brien, P. & Pickett, N. L. (2001). *Chem. Mater.* **13**, 3843–3858.
Wang, Z. L., Kong, X. Y., Ding, Y., Gao, P., Hughes, W. L., Yang, R. & Zhang, Y. (2004). *Adv. Funct. Mater.* **14**, 943–956.